

# FAPi PET/CT for assessment and visualisation of active myositis-related interstitial lung disease: a prospective observational pilot study



Kastriot Kastrati,<sup>a</sup> Thomas S. Nakuz,<sup>b</sup> Oana C. Kulterer,<sup>b</sup> Irina Gefßl,<sup>a</sup> Elisabeth Simader,<sup>a</sup> Daniel Mrak,<sup>a</sup> Michael Bonelli,<sup>a</sup> Hans Peter Kiener,<sup>a</sup> Florian Prayer,<sup>c</sup> Helmut Prosch,<sup>c</sup> Daniel Aletaha,<sup>a</sup> Werner Langsteiger,<sup>b</sup> Tatjana Traub-Weidinger,<sup>b</sup> Stephan Blüml,<sup>a</sup> Helga Lechner-Radner,<sup>a</sup> Marcus Hacker,<sup>b</sup> and Peter Mandl<sup>a,\*</sup>



<sup>a</sup>Division of Rheumatology, Department of Internal Medicine III, Medical University of Vienna, Vienna, Austria

<sup>b</sup>Division of Nuclear Medicine, Department of Biomedical Imaging and Image-guided Therapy, Medical University of Vienna, Vienna, Austria

<sup>c</sup>Division of General and Paediatric Radiology, Department of Biomedical Imaging and Image-guided Therapy, Medical University of Vienna, Vienna, Austria

## Summary

**Background** Interstitial lung disease (ILD) is a common manifestation of idiopathic inflammatory myopathies (IIM) and a substantial contributor to hospitalisation, increased morbidity, and mortality. In-vivo evidence of ongoing tissue remodelling in IIM-ILD is scarce. We aimed to evaluate fibroblast activation in lungs of IIM-patients and control individuals using <sup>68</sup>Ga-labelled inhibitor of Fibroblast-Activation-Protein (FAPi) based positronic emission tomography and computed tomography imaging (PET/CT).

**Methods** In this prospective observational pilot study, consecutive patients with IIM and participants without rheumatic conditions or ILD serving as a control group were recruited at the Medical University of Vienna, Austria, and underwent FAPi PET/CT imaging. Standard-of-care procedures including clinical examination, assessment of severity of dyspnoea, high-resolution computed tomography (HR-CT), and pulmonary function testing (PFT) were performed on all patients with IIM at baseline and for patients with IIM-ILD at follow-up of 12 months. Baseline pulmonary FAPi-uptake was assessed by the maximum (SUV<sub>max</sub>) and mean (SUV<sub>mean</sub>) standardized uptake values (SUV) over the whole lung (wl). SUV was corrected for blood pool background activity and target-to-background ratios (TBR) were calculated. We compared pulmonary FAPi-uptake between patients with IIM-ILD and those without ILD, as well as controls, and correlated baseline FAP-uptake with standard diagnostic tools such as HR-CT and PFT. For predictive implications, we investigated whether patients with IIM and progressive ILD exhibited higher baseline FAPi-uptake compared to those with stable ILD. Metrics are reported as mean with standard deviation ( $\pm$ SD).

**Findings** Between November 16, 2021 and October 10, 2022, a total of 32 patients were enrolled in the study. Three participants from the control group were excluded due to cardiopulmonary disease. In individuals with IIM-ILD (n = 14), wTBR<sub>max</sub> and wTBR<sub>mean</sub> were significantly increased as compared with both non-ILD-IIM patients (n = 5) and the control group (n = 16): wTBR<sub>max</sub>: 2.06  $\pm$  1.04 vs. 1.04  $\pm$  0.22 (p = 0.019) and 1.08  $\pm$  0.19 (p = 0.0012) and wTBR<sub>mean</sub>: 0.45  $\pm$  0.19 vs. 0.26  $\pm$  0.06 (p = 0.025) and 0.27  $\pm$  0.07 (p = 0.0024). Similar values were observed in wTBR<sub>max</sub> or wTBR<sub>mean</sub> between non-ILD IIM patients and the control group. Patients with progressive ILD displayed significantly enhanced wTBR<sub>max</sub> and wTBR<sub>mean</sub> values at baseline compared to patients with stable ILD: wTBR<sub>max</sub>: 1.30  $\pm$  0.31 vs. 2.63  $\pm$  1.04 (p = 0.0084) and wTBR<sub>mean</sub>: 0.32  $\pm$  0.08 vs. 0.55  $\pm$  0.19 (p = 0.021). Strong correlations were found between FAPi-uptake and disease extent on HR-CT (wTBR<sub>max</sub>: R = 0.42, p = 0.07; wTBR<sub>mean</sub>: R = 0.56, p = 0.013) and severity of respiratory symptoms determined by the New York Heart Association (NYHA) classification tool (wTBR<sub>max</sub>: R = 0.52, p = 0.022; wTBR<sub>mean</sub>: R = 0.59, p = 0.0073). Further, pulmonary FAPi-uptake showed inverse correlation with forced vital capacity (FVC) (wTBR<sub>max</sub>: R = -0.56, p = 0.012; wTBR<sub>mean</sub>: R = -0.64, p = 0.0033) and diffusing capacity of the lungs for carbon monoxide (DLCO) (wTBR<sub>max</sub>: R = -0.52, p = 0.028; wTBR<sub>mean</sub>: R = -0.68, p = 0.0017).

**Interpretation** Our study demonstrates higher fibroblast activation in patients with IIM-ILD compared to non-ILD patients and controls. Intensity of pulmonary FAPi accumulation was associated with progression of ILD.

eClinicalMedicine  
2024;72: 102598  
Published Online xxx  
<https://doi.org/10.1016/j.eclinm.2024.102598>

\*Corresponding author.

E-mail address: [peter.mandl@meduniwien.ac.at](mailto:peter.mandl@meduniwien.ac.at) (P. Mandl).

Considering that this study was carried out on a small population, FAPI PET/CT may serve as a useful non-invasive tool for risk stratification of lung disease in IIM.

**Funding** The Austrian Research Fund.

**Copyright** © 2024 The Authors. Published by Elsevier Ltd. This is an open access article under the CC BY-NC-ND license (<http://creativecommons.org/licenses/by-nc-nd/4.0/>).

**Keywords:** Idiopathic inflammatory myopathy; Interstitial lung disease; Fibrosis; Fibroblast activation

### Research in context

#### Evidence before this study

We conducted a comprehensive literature review and searched PubMed for studies published until November 14, 2023, using search terms including idiopathic inflammatory myopathy (IIM), myositis, interstitial lung disease (ILD), progression, biomarkers, Fibroblast-Activation-Protein (FAPI) based positron emission tomography and computed tomography imaging, or FAPI-PET, with search terms found in abstracts or titles. We found a case report involving a female dermatomyositis patient highlighted elevated FAPI activity correlating with pulmonary fibrosis. However, the body of evidence regarding the use of FAPI-based imaging in assessing ILD in the context of IIM is scarce.

#### Added value of this study

In this proof-of-concept study, we show that patients with IIM-ILD have significantly elevated gallium 68 (<sup>68</sup>Ga)-labelled inhibitor of FAPI uptake, which specifically depicts activated fibroblasts *in vivo* in these patients as compared to those without ILD and control individuals. The intensity of FAPI-

uptake in the lungs significantly correlates with distinct clinical parameters and the severity of respiratory symptoms. FAPI uptake correlates with disease extent on high-resolution computed tomography (HR-CT), moreover we observe significant negative correlation between <sup>68</sup>Ga-labelled FAPI uptake and pulmonary function tests (PFT) and positive correlation with systemic inflammation parameters at baseline. Myositis patients with progressive ILD, defined as either increase in respiratory symptoms, progression in HR-CT, deterioration in PFT or escalation of therapy within one year, exhibit significantly higher whole-lung FAPI-uptake at baseline.

#### Implications of all the available evidence

Considering that this observational study conducted on a small population, quantification of fibroblast activation by <sup>68</sup>Ga-labelled FAPI PET/CT may refine predictions of the clinical trajectory of individuals with myositis-associated ILD. This study provides first evidence for the usefulness of this non-invasive imaging technique in risk stratification.

## Introduction

Idiopathic inflammatory myopathies (IIM) are rare autoimmune disorders marked by skeletal muscle weakness, muscular atrophy, and physical disability. Extra-muscular complications are frequent, including arthritis, cardiac, microvascular, dermatological, or pulmonary involvement, highlighting the systemic nature of IIM.<sup>1</sup> The extent and pattern of organ involvement varies greatly among patients with IIM. Interstitial lung disease (ILD) is a common and devastating manifestation occurring in up to 78% of patients with IIM. ILD significantly contributes to hospitalisation, excess morbidity, and mortality.<sup>2</sup> In particular, certain IIM subtypes such as antisynthetase syndrome (ASyS) or clinically amyopathic dermatomyositis with autoantibodies against melanoma differentiation-associated protein are characterised by high incidence of ILD, which may be the sole manifestation of the disease.<sup>3</sup> However, in other subtypes, such as overlap syndromes, patients are often not spared from ILD.<sup>4</sup>

Current treatment strategies in IIM-ILD include immunosuppressive as well as antifibrotic agents.<sup>5</sup> Nevertheless, the management of IIM-ILD poses a

formidable challenge. Although traditional biomarkers such as distinct myositis-specific autoantibodies, elevated acute phase reactants or serum ferritin are associated with disease progression, the disease course remains difficult to predict.<sup>6,7</sup> Furthermore, progression of pulmonary involvement may occur under immunosuppressive therapy, and the course of pulmonary disease in individual patients even of the same IIM subtype is variable.<sup>8</sup> In current clinical practice, risk stratification and monitoring of ILD is determined by clinical symptoms (progressive non-productive cough, exertional dyspnoea and reduced exercise tolerance), pulmonary function testing (PFT), and lung morphology assessed on high-resolution computed tomography (HR-CT).<sup>9</sup> Although HR-CT depicts the extent of lung involvement, it cannot distinguish between ongoing active fibrotic processes and fibrotic remodelling that already took place. From a pathophysiological perspective, the differentiation of activated fibroblasts into myofibroblasts, which induces lung remodelling and fibrosis plays a key role in ILD.<sup>10–12</sup> Activated fibroblasts differ from their quiescent counterparts in their gene expression profile. A surface propyl-specific serine protease

named fibroblast activation protein (FAP) is one of such differentially expressed genes.<sup>13</sup> In the past few years, it has emerged as a theranostic target for radionuclides that act as FAP inhibitors (FAPi).<sup>14</sup> Positron emission tomography (PET) imaging utilising FAPi-based tracers have made headway in the last decade in oncology.<sup>15</sup> Moreover, there is increasing evidence also in the field of rheumatic and musculoskeletal diseases (RMD) for its value in visualising inflammation driven tissue fibrosis, such as in IgG4-related disease.<sup>16</sup> With regard to lung involvement in RMDs, accumulation of gallium 68 (<sup>68</sup>Ga)-FAPi-04 was demonstrated in patients with systemic sclerosis (SSc)-associated ILD *in vivo* and the intensity of FAPi-uptake correlated with pulmonary disease progression.<sup>17</sup> While the application of FAPi in IIM remains scarce, a recent case report involving a female dermatomyositis patient highlighted elevated FAPi activity correlating with pulmonary fibrosis.<sup>18</sup>

In light of these advancements, we aimed to assess the utility of [<sup>68</sup>Ga]<sup>68</sup>Ga-DATA5m.SA.FAPi-PET/CT for distinguishing patients with IIM with or without pulmonary involvement and investigated whether the extent of FAPi-uptake correlates with disease progression by using PFT, HR-CT, clinical symptoms, and escalation of treatment as the reference standard.

## Methods

### Study design and participants

In this single-centre pilot study, patients with a clinically established diagnosis of IIM according to the EULAR/ACR classification criteria for adult and juvenile IIM,<sup>19</sup> ASyS according to the Connors criteria,<sup>20</sup> and immune-mediated necrotising myopathy (IMNM) meeting the 2017 European Neuromuscular Centre classification (ENMC) criteria<sup>21</sup> were recruited consecutively between November 16, 2021, and October 10 2022, from the outpatient clinic of the Department of Rheumatology of the Medical University of Vienna, a tertiary centre for RMDs in Austria. Additional inclusion criteria consisted of the following: a) availability of HR-CT to confirm or rule out IIM-ILD, b) presence of recent PFT, c) written informed consent prior to enrolment in the study, and d) age of ≥18 years when signing informed consent. The following exclusion criteria were applied: a) non-IIM-related pulmonary disease such as sarcoidosis, pulmonary infection or history of COVID-19 pneumonia, malignancy, or prior lung surgery, b) breastfeeding or pregnancy, and c) inability to give informed consent. Patients were divided into two groups, those with and without presence of ILD based on HR-CT findings. To ensure consistency and reliability of the assessments between the groups, patients eligible for transcatheter aortic valve implantation (TAVI) without history or presence of any RMD or any pulmonary disease including acute infection or cardiac decompensation were recruited consecutively (not

age- or gender-matched) at the Department of Cardiology at the Medical University of Vienna as control individuals. As this is a pilot study, no formal sample size calculation was conducted. The methodology and reporting of this study adhere to the Strengthening the Reporting of Observational Studies in Epidemiology (STROBE) guidelines. This prospective study was approved by the Ethics Committee of the Medical University of Vienna (identification no. 1400/2020). Informed consent was obtained from all participants prior to their inclusion in the study, following institutional ethical guidelines.

### Assessment and outcome measures

With regards to patients with IIM, clinical data were obtained from our prospective myositis-register as well as electronic medical records (EMR) including the following: laboratory parameters (acute phase parameters including C-reactive protein [CRP] and erythrocyte sedimentation rate [ESR], serum levels of muscle enzymes including creatine kinase, auto-antibodies including antinuclear antibodies [ANA], myositis-specific and myositis-associated antibodies), imaging results (HR-CT of the chest, clinical IIM-features (skin lesions, arthritis, pulmonary-, gastrointestinal-, myocardial involvement), clinical assessments (PFTs, Manual Muscle Testing [MMT] scale, severity of respiratory symptoms according to the New York Heart Association [NYHA] classification tool,<sup>22</sup> and disease activity core set measures including patient and physician global disease activity, extra-muscular disease activity assessed by numerical rating scale [NRS]) and information on start/escalation of immunosuppressive or antifibrotic agents. All recruited patients with IIM underwent [<sup>68</sup>Ga]<sup>68</sup>Ga-DATA5m.SA.FAPi-PET/CT imaging, as well as PFTs at baseline. In line with the recommendations,<sup>4</sup> PFTs were repeated every six months, while HR-CT imaging was performed annually in patients with IIM-ILD. HR-CT scans were used to determine presence of ILD and to perform semiquantitative scoring of ILD extent.

For predictive implications in this at risk population, patients with IIM-ILD were grouped into “progressors” and “non-progressors” based on an adaption of the original criteria proposed by ATS/ERS/JRS/ALAT 2022 definition for progressive pulmonary fibrosis: a) deterioration in PFT in accordance with defined as ≥5% absolute decline in FVC and/or ≥10% absolute decline in percentage of predicted haemoglobin adjusted diffusing capacity of the lung for carbon monoxide (DLCO) occurring within one year and without alternative explanation, or disease progression on CT scan<sup>23</sup>; this was supplemented by an additional criterion: b) and/or necessity for intensification of immunosuppressive and/or anti-fibrotic therapy due to worsening respiratory symptoms (including hospitalisation because of respiratory distress or ILD exacerbation) at the discretion of the treating clinician. Therapy intensification was

defined as the initiation of an additional immunosuppressive (systemic glucocorticoids [GC] or at least a doubling of the existing daily GC dosage or immunomodulatory regimen), antifibrotic agent or initiation/escalation of long-term supplemental oxygen therapy (LTOT) during the observational time frame. Non-progressive ILD was defined if none of the above-mentioned criteria were fulfilled.

### **[<sup>68</sup>Ga]<sup>68</sup>Ga-DATA5m.SA.FAPi-PET/CT protocol and procedures**

A mean dosage around 2 MBq/kg body weight of [<sup>68</sup>Ga]<sup>68</sup>Ga-DATA5m.SA.FAPi was administered to all participants in both groups. Sixty minutes after the tracer administration, participants received CT imaging, followed by whole-body PET scan. Image interpretation was conducted using Hybrid 3D HERMES software (Stockholm, Sweden).

We used the radiopharmaceutical [<sup>68</sup>Ga]<sup>68</sup>Ga-DATA5m.SA.FAPi, a squaric-acid, quinolone-based molecule with in vitro FAP inhibiting functions, demonstrating high diagnostic performance and favourable tracer kinetics for both imaging and potential therapeutic applications for all PET examinations within this study.<sup>24</sup> The synthesis of the ligand DATA5m.SA.FAPi was performed and provided by the Johannes Gutenberg University Mainz, Germany. Radiolabelling of the applied tracer was carried out at the Department of Biomedical Imaging and Image-guided Therapy of the Medical University of Vienna, Austria, according to predefined methodology.<sup>25</sup>

### **Image interpretation and analysis**

Analyses of the HR-CT examinations of the chest were independently conducted by two experienced radiologists in lung imaging. Both radiologists were blinded to disease-related clinical data, imaging reports, PFT results and [<sup>68</sup>Ga]<sup>68</sup>Ga-DATA5m.SA.FAPi-PET/CT imaging reports. HR-CT scans were investigated for the presence and overall extent of ILD-related lung abnormalities and were semi-quantitatively scored by applying the visual staging system proposed by Goh et al.<sup>26</sup> comprising the following variables: total disease extent, and proportion of ground glass (defined as increased opacity of pulmonary parenchyma with preserved bronchial and vascular margins). In brief, the extent of lung involvement was estimated in five pre-defined sections (1. Origin of great vessels; 2. Main carina; 3. Pulmonary venous confluence, 4. Halfway between the third and fifth section, 5. Immediately above the right-hemidiaphragm) in 5% increments. An additional assessment for bronchial wall thickening, bronchiectasis, extent of consolidation (defined as homogeneous increase in parenchymal attenuation obscuring the margins of vessels and airway walls, optionally accompanied by air bronchograms), reticular pattern (characterized by thickening of interlobular or intralobular septa), honeycombing (presenting

in the form of clustered cystic air spaces, typically of comparable diameters) and emphysema, respectively, pursuant to the Fleischner Society's glossary of terms for thoracic imaging<sup>27</sup> was performed. Two-reader consensus dichotomous- (visually discernible presence/absence of ILD) and semiquantitative HR-CT scores were calculated for each patient with IIM.

All [<sup>68</sup>Ga]<sup>68</sup>Ga-DATA5m.SA.FAPi-PET/CT images were independently assessed in a random order by two experienced nuclear medicine physicians, who were blinded to clinical data as well as disease-specific information, including the results of PFTs and HR-CT. In case of uncertainties, the results were discussed with a senior nuclear medicine physician. Evidence of any focal uptake higher than the surrounding background within the lung parenchyma was considered pathological. Pulmonary tracer uptake was quantified by measuring the maximal standardised uptake (SUV) value (SUV<sub>max</sub>) and mean SUV (SUV<sub>mean</sub>). The blood pool SUV was measured by assessing the SUV<sub>mean</sub> in the ascending aorta at time of imaging with a fixed volume of 10 ml. Using the measured SUV<sub>mean</sub>, blood pool-corrected target-to-background (TBR) ratios were established. Whole-lung delineation was executed using CT-based HU-thresholds. CT-acquisition during shallow breathing and fibrotic changes in the lungs necessitated an individualised approach to the thresholds. CT-based delineations were subsequently copied to the corresponding PET-data for measurement of SUV values.

### **Statistical analysis**

Statistical analyses were performed using SPSS Statistics for Windows (version 27.0, IBM) and "R" version 4.2.2 (R Development Core Team, Vienna, Austria). The package "ggplot2" was utilized for creating plots. GraphPad Prism version 6 was used for the graphical presentation of the data. After assessment of the distribution visually and by applying the Shapiro–Wilk test, continuous variables are expressed as mean with standard deviation (SD) or median with interquartile range (IQR). Categorical data are depicted using absolute frequencies with percentages. Comparison between different groups was carried out by either t-test and one-way analysis of variance (ANOVA) for parametric or by Kruskal–Wallis-test for non-parametric data. Categorical variables were analysed using Chi-Square or Fisher's exact test. 95% confidence intervals for the difference in SUV magnitude between non-ILD vs. ILD, ILD vs. control, and non-ILD vs. control were reported. Associations between <sup>68</sup>GaFAPi-derived TBR<sub>max</sub> as well as TBR<sub>mean</sub> measurements, and continuous variables were assessed via Spearman rank correlation coefficient (R). A p-value of ≤0.05 was considered indicative for statistical difference. In addition to comparing PFT values (FVC and DLCO) and total disease extent on HR-CT between non-progressors and progressors, logistic regression analyses were performed to assess the

predictive value of FAPI-uptake ( $w\text{TBR}_{\text{max}}$  and  $w\text{TBR}_{\text{mean}}$ ) in conjunction with baseline PFT parameters and disease extent on HR-CT for predicting disease progression after one year. For each covariate, logistic regression models were constructed with and without the addition of SUV parameters. The performance of each model was evaluated using the Akaike Information Criterion (AIC) and R-squared values.

### Role of the funding source

The funder of the study had no role in study design, data collection, data analysis, data interpretation, or writing of the report. KK, TSN and PM had full access to the dataset and had final responsibility for the decision to submit for publication.

## Results

### Participant characteristics

We recruited a total of 19 participants with IIM (mean age  $52.6 \pm 15.3$  years; 11 female) and a total of 19 control individuals (mean age  $78.8 \pm 3.8$  years; 14 female). Three participants from the control group were excluded; two patients due to aortic stenosis related cardiac decompensation with significantly increased natriuretic peptide levels and one patient due to infectious pulmonary disease (Fig. 1). Consequently, 16 patients from the control group were included in the analysis. Key characteristics of the participants including demographic and clinical data are shown in Table 1.

A total of 14 out of the 19 patients with IIM enrolled suffered from ILD, primarily from ASyS. In patients with myositis, the average disease duration at the time of FAPI imaging was  $3.1 \pm 4.3$  years. Patients with IIM-related ILD exhibited a pattern of lung involvement on CT corresponding either to nonspecific interstitial pneumonia (NSIP;  $n = 5$ , 35.7%), organising pneumonia (OP;  $n = 4$ , 28.6%), a combination of both ( $n = 4$ , 28.6%), or usual interstitial pneumonia (UIP;  $n = 1$ , 7.7%). Except for two patients, all patients with IIM received concomitant immunosuppressive or anti-fibrotic medication at baseline, i.e. timepoint of FAPI PET/CT imaging (Table 1). Detailed myositis-related disease features among patients with IIM are depicted in Supplementary Table S1, stratified by IIM-ILD and non-ILD cases.

### Pulmonary FAPI-uptake

Whole-lung (wl)  $^{68}\text{Ga}$ -FAPI-derived  $\text{TBR}_{\text{max}}$  was significantly increased in the ILD group as compared to both non-ILD IIM patients and the control group:  $w\text{TBR}_{\text{max}}$ :  $2.06 \pm 1.04$  vs.  $1.04 \pm 0.22$  (difference  $-1.02$ , 95% CI:  $-1.89$ ,  $-0.14$ ;  $p = 0.019$ ) and  $1.08 \pm 0.19$  (difference  $0.98$ , 95% CI:  $0.37$ ,  $1.59$ ;  $p = 0.0012$ ) respectively (Fig. 2A). Moreover,  $w\text{TBR}_{\text{mean}}$  was significantly greater in patients with IIM-ILD as compared to patients with IIM without lung abnormalities ( $0.45 \pm 0.19$  vs.  $0.26 \pm 0.06$  [difference  $-0.19$ , 95% CI:  $-0.36$ ,  $-0.02$ ;  $p = 0.025$ ]) and control individuals ( $0.27 \pm 0.07$  [difference  $0.18$ , 95% CI:  $0.06$ ,  $0.30$ ;  $p = 0.0024$ ]) (Fig. 2B). We found similar

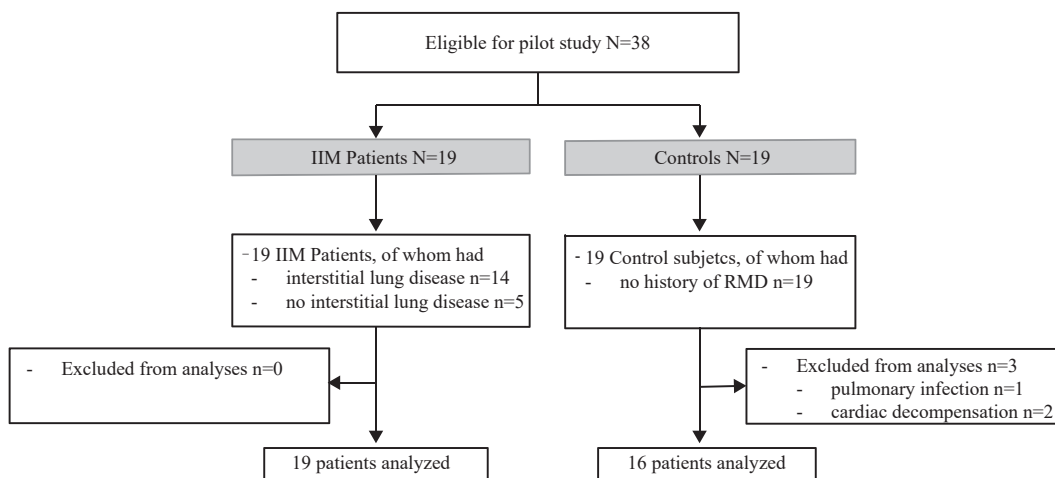


**Fig. 1: Study flow diagram indicating assessment for eligibility for inclusion for pilot study.**  $N = 19$  adult patients with idiopathic inflammatory myopathy (IIM) and recently (not older than 4 weeks) available HR-CT and PFT were recruited and included in the study, of whom  $n = 14$  exhibited an interstitial lung disease (ILD). Every IIM patient completed the study.  $N = 14/14$  with IIM-related ILD completed 1-year follow-up as planned. A total of 19 participants (mean age  $79$  years  $\pm 3.8$  [SD]; 14 female) eligible for transcatheter aortic valve implantation (TAVI) were recruited as controls. Three participants from the control group were excluded due to cardiopulmonary disease:  $n = 2$  patients due to aortic stenosis related cardiac decompensation with significantly increased natriuretic peptide levels and signs of pulmonary congestion and oedema;  $n = 1$  patient due to infectious pulmonary disease. Abbreviations: N/n, number; IIM, idiopathic inflammatory myopathy; TAVI, transcatheter aortic valve implantation; RMD, rheumatic and musculoskeletal disease; HR-CT, high-resolution computed tomography; PFT, pulmonary function test.

	IIM patients	Controls
No. (n)	19	16
Sex		
Female	11 (57.9%)	12 (75%)
Male	8 (42.1%)	4 (25%)
Mean age (years ± SD)	52.6 ± 15.3	78.8 ± 3.8
Ethnicity (Caucasian)	18 (94.7%)	16 (100%)
Mean disease duration (years ± SD)	3.1 ± 4.3	-
Disease subtype		
Antisynthetase syndrome	11 (57.9%)	-
Dermatomyositis	3 (15.8%)	-
Overlap myositis	3 (15.8%)	-
Immune-mediated necrotizing myopathy	2 (10.5%)	-
Interstitial lung disease (ILD) on HR-CT		
Yes	14 (73.7%)	-
ILD-subtype		
NSIP	5 (35.7%)	-
UIP	1 (7.7%)	-
OP	4 (28.6%)	-
NSIP and OP	4 (28.6%)	-
Autoantibodies		
Aminoacyl-tRNA synthetase	11 (57.9%)	-
Ro-52	3 (15.8%)	-
MDA5	2 (10.5%)	-
Mi-2	1 (5.3%)	-
Seronegative	2 (10.5%)	-
Immunosuppressive/antifibrotic therapy		
Corticosteroid	8 (42.1%)	-
Hydroxychloroquine	1 (5.3%)	-
Methotrexate	2 (10.5%)	-
Mycophenolate mofetil	9 (47.4%)	-
Rituximab	1 (5.3%)	-
Intravenous immunoglobulin	5 (26.3%)	-
Nintedanib	3 (15.8%)	-
No treatment	2 (10.5%)	16 (100%)
Acute phase parameters (mean ± SD)		
CRP in mg/dL	0.4 ± 0.5	-
ESR in mm/h	21.2 ± 24.5	-
Pulmonary function tests (mean ± SD)		
FVC %	81.3 ± 22.5	-
DLCO %	67.7 ± 19.8	-
Corresponding HR-CT findings (mean ± SD)		
Total disease extent (%)	25 ± 24.8	0

IIM, idiopathic inflammatory myopathy; No./n, number; SD, standard deviation; NSIP, nonspecific interstitial pneumonia; UIP, usual interstitial pneumonia; OP, organising pneumonia; CRP, C-reactive protein; ESR, erythrocyte sedimentation rate; FVC (% predicted), forced vital capacity; DLCO (% predicted), diffusion capacity of the lungs for carbon monoxide; HR-CT, high-resolution computed tomography.

**Table 1: Demographic and clinical characteristics of participants at baseline (timepoint of FAPI imaging).**

values in both wITBR<sub>max</sub> (1.04 ± 0.22 vs. 1.08 ± 0.19 [difference -0.04, 95% CI: -0.89, 0.82; p = 0.99]) and wITBR<sub>mean</sub> (0.26 ± 0.06 vs. 0.27 ± 0.07 [difference -0.01, 95% CI: -0.18, 0.16; p = 0.98]) between non-ILD myositis patients and the control group.

### Overall extent and morphological patterns of ILD on computed tomography

Whole-lung TBR<sub>max</sub> and TBR<sub>mean</sub> strongly correlated with the total parenchymal disease extent on HR-CT at baseline (wITBR<sub>max</sub>: R = 0.42, p = 0.07; wITBR<sub>mean</sub>: R = 0.56, p = 0.013). Reticular infiltrates, which constitute a CT-morphologic printout of fibrotic lung disease, also showed strong correlation with magnitude of [<sup>68</sup>Ga]<sup>68</sup>Ga-DATA5m.SA.FAPi-PET parameters (wITBR<sub>max</sub>: R = 0.45, p = 0.05; wITBR<sub>mean</sub>: R = 0.61, p = 0.0052). In contrast, no correlation could be identified regarding the extent of consolidations (wITBR<sub>max</sub>: R = 0.2, p = 0.42; wITBR<sub>mean</sub>: R = 0.25, p = 0.31) (Fig. 3). Likewise, as only one patient exhibited a pattern corresponding to UIP, no association with the extent of honeycombing could be confirmed, likely due to the small sample size (wITBR<sub>max</sub>: R = 0.22, p = 0.38; wITBR<sub>mean</sub>: R = 0.3, p = 0.21).

### Pulmonary function tests

The overall FAPi-uptake throughout the entire lung, both wITBR<sub>max</sub> and wITBR<sub>mean</sub>, displayed strong negative correlation with forced vital capacity (FVC) (wITBR<sub>max</sub>: R = -0.56, p = 0.012; wITBR<sub>mean</sub>: R = -0.64, p = 0.0033) (Fig. 4). Baseline DLCO correlated inversely with wITBR<sub>max</sub> (R = -0.52, p = 0.028) as well as with wITBR<sub>mean</sub> (R = -0.68, p = 0.0017) (Fig. 4).

### Severity of dyspnoea, acute-phase reactants and disease activity core set measures

Whole lung maximum and mean TBR in the lungs strongly correlated with the severity of dyspnoea as per NYHA classification (Supplementary Fig. S1). We observed correlations for pulmonary FAPi-uptake also with acute phase reactants. In particular for ESR and CRP, we identified clear correlations between the extent of the FAPi-uptake (Supplementary Fig. S2). Furthermore, a strong correlation was evident between pulmonary FAPi-uptake and core set measures including patient and physician global disease activity, as well as extra-muscular disease activity. Nevertheless, no correlation was found with manual muscle testing scores or CK levels in serum (Supplementary Fig. S3).

### Risk stratification and predictive implications

Patients with IIM-ILD who were not at risk for progression (non-progressors, n = 6/14; 42.9%) had significantly lower whole-lung FAPi uptake in relation to the blood pool at baseline as compared to progressors (n = 8/14; 57.1%) (wITBR<sub>max</sub>: 1.30 ± 0.31 vs. 2.63 ± 1.04 [difference 1.33, 95% CI: 0.44, 2.21; p = 0.0084]; wITBR<sub>mean</sub>: 0.32 ± 0.08 vs. 0.55 ± 0.19 [difference 0.23, 95% CI: 0.04, 0.42; p = 0.021]) (Fig. 5A and B). Supplementary Table S2 provides detailed information regarding the distribution of patients with IIM-ILD meeting each criterion for stable and progressive disease. Furthermore, logistic regression analyses revealed

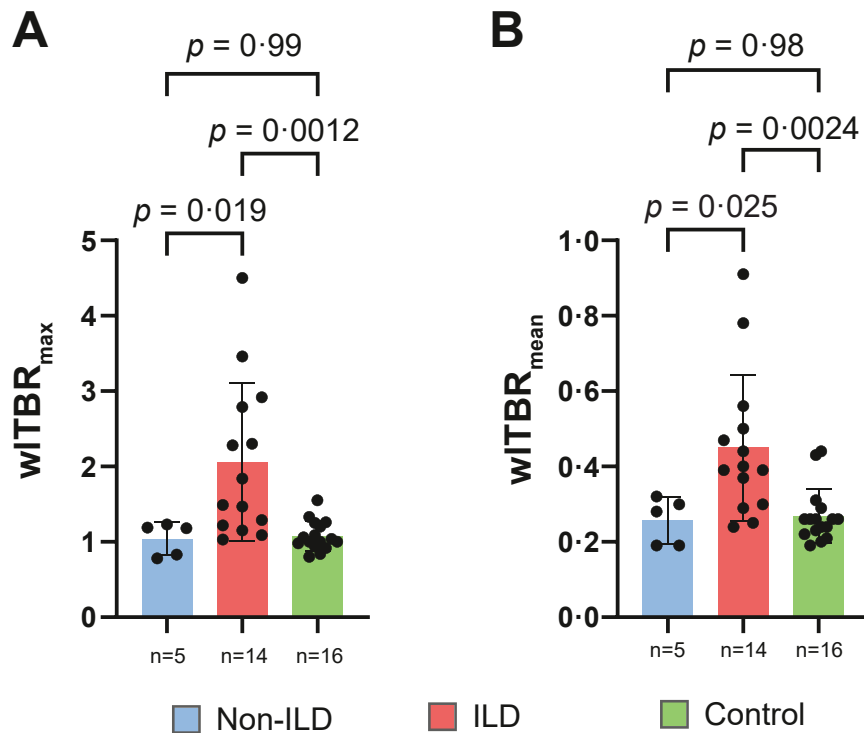


**Fig. 2: Maximum and mean  $[^{68}\text{Ga}]^{168}\text{Ga}$ -DATA5m.SA.FAPI-derived SUV in the lungs of patients with IIM and controls in relation to blood pool.** Mean (SD) whole-lung maximum target-to-background ratio (A); mean value (SD) of whole-lung mean target-to-background ratio in myositis patients with or without interstitial lung disease and control individuals (B). Abbreviations: ILD, interstitial lung disease; wITBR<sub>max</sub>, whole-lung maximum target-to-background ratio; wITBR<sub>mean</sub>, whole-lung mean target-to-background ratio; SD, standard deviation.

increasing predictive capability of conventional measures such as PFT (FVC and DLCO), and baseline HR-CT extent in conjunction with pulmonary FAPI-uptake for assessing disease progression. The outcomes of these analyses, summarized in [Supplementary Table S3](#), indicate that integrating FAPI-uptake with standard methods of assessment led to improvements in identifying patients at risk for progression.

## Discussion

In this proof-of-concept study, we show that patients with IIM-ILD had significantly elevated tracer uptake, which specifically depicts activated fibroblasts *in vivo* as compared to those without ILD and controls. We demonstrate that increased FAPI-uptake can discriminate patients with IIM and ILD from those without ILD. In addition, we show that the intensity of FAPI-accumulation in the lungs correlates with distinct clinical parameters and the severity of the respiratory symptoms in patients with IIM-ILD. On the one hand, there was a significant correlation with disease extent on HR-CT, on the other hand, we observed a correlation with PFTs and systemic inflammation parameters at baseline. Importantly, we could also show that patients

with progressive IIM-ILD show elevated FAPI-uptake as compared to those with stable disease. This is in line with previous studies looking at other autoimmune RMDs.<sup>17</sup>

Currently, assessment of ILD in patients with IIM relies on PFTs, measuring the extent of the disease through HR-CT, and respiratory symptoms. However, PFT results correlate only partially with HR-CT scores and pattern. Furthermore, PFT are more sensitive to change as compared to HR-CT abnormalities.<sup>28</sup> Overall, the current assessment standards require an extended period of monitoring to identify alterations and are not capable to depict disease-driven pulmonary remodelling at the time of assessment. Our study not only demonstrates significant correlation between FAPI-uptake and PFTs but also with the extent of lung disease observed on HR-CT. Additionally, patients with heightened FAPI-uptake exhibited more severe respiratory symptoms. This interrelation between FAPI-uptake, PFT results, HR-CT scores, and severity of respiratory symptoms highlights the content validity of FAPI PET/CT and its ability to comprehensively reflect activity of IIM-ILD. Myositis patients with progressive ILD (defined as increase in respiratory symptoms, progression on HR-CT, decline in lung function based on current

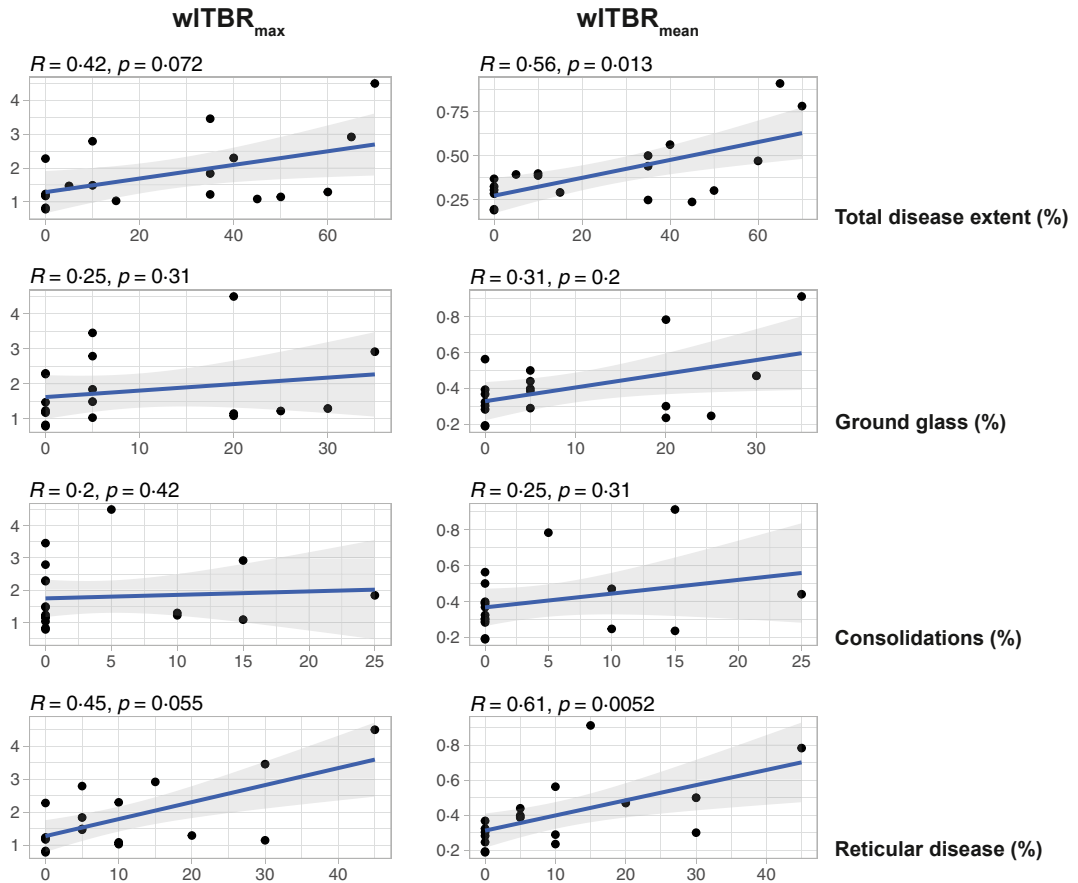


**Fig. 3: Pulmonary maximum and mean  $[^{68}\text{Ga}]^{68}\text{Ga}$ -DATA5m.SA.FAPi-derived SUV corrected for the blood pool of patients with IIM and correlations with CT-morphologic extent of total disease and ILD-specific features.** Whole-lung maximum and mean target-to-background ratios in myositis patients in relation to semi-quantitative scores of the parenchymal total disease extent (%), extent of ground glass opacities (%), extent of consolidations (%), extent of reticular disease (%) and honeycombing (%) on HR-CT. Abbreviations: wITBR<sub>max</sub>, whole-lung maximum target-to-background ratio; wITBR<sub>mean</sub>, whole-lung mean target-to-background ratio; R, Spearman's correlation coefficient rho.

recommendations, and/or need of treatment escalation within one year) exhibited significantly higher whole-lung FAPi-uptake at baseline, alluding to the potential of FAPi PET/CT in identifying patients at risk for progression. In our cohort only one patient showed progressive HR-CT findings, while the rest remained stable on HR-CT. However, patients with elevated FAPi-uptake experienced worsening in lung function, increased respiratory symptoms, or required intensified therapy. This discrepancy suggests a higher sensitivity of FAPi PET/CT in predicting the course of pulmonary disease compared to conventional HR-CT scans. By capturing the patient's pulmonary condition in a holistic way, FAPi PET/CT may therefore improve identifying patients at risk for progression and serve as a tool for comprehensive and dynamic disease monitoring.

As of yet, only a small number of studies have investigated the use of FAPi PET/CT for ILD. It was recently shown in vitro that FAP-expression is

significantly upregulated during the early phase of profibrotic cytokine-mediated fibroblast activation, and that FAP-positive fibroblasts produce collagen. Immunohistochemistry revealed that FAP-expression correlated closely with an abundance of fibroblastic foci in human lung biopsy sections of patients with ILD.<sup>29</sup> Mouse models have demonstrated the significance of FAP-expression in pulmonary fibrosis for diagnosis as well as a potential, novel therapy. CT was incapable of correctly assessing fibrotic changes in mouse models with bleomycin-induced pulmonary fibrosis, while a FAPi PET tracer enabled the detection of pulmonary fibrosis and even gauging the activity of fibrogenesis that correlated with the histological work-up.<sup>30</sup> The antifibrogenic effect of a FAP-inhibitor (PT100) was confirmed in bleomycin-induced mouse models of pulmonary fibrosis.<sup>31</sup>

Our study has several limitations. First, it was carried out on a small population, which also included



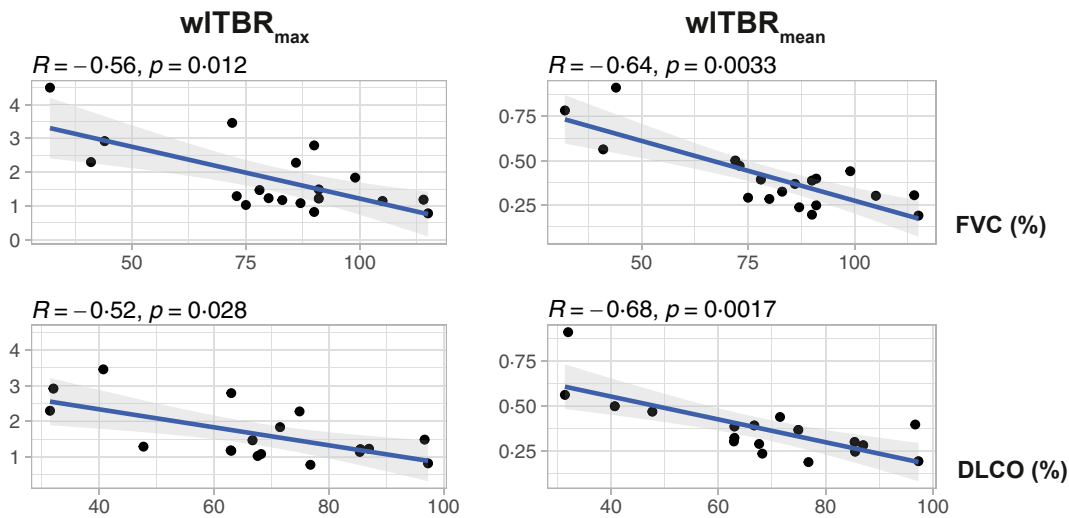


**Fig. 4: Pulmonary maximum and mean  $[^{68}Ga]^{68}Ga$ -DATA5m.SA.FAPI-PET-derived SUV corrected for the blood pool of patients with IIM in relation to pulmonary function tests (PFTs) at baseline.** PFTs (% predicted) showed negative correlations with whole-lung maximum and mean target-to-background ratios. Abbreviations:  $wITBR_{max}$ , whole-lung maximum target-to-background ratio;  $wITBR_{mean}$ , whole-lung mean target-to-background ratio; FVC (% predicted), forced vital capacity; DLCO (% predicted), diffusing capacity of the lungs for carbon monoxide; R, Spearman's correlation coefficient rho.

participants with different types of IIM at various stages of the disease. Due to the small sample size, possible differences, such as those between the control group and patients without ILD, may have gone undetected. Another important limitation is the scanning protocol for the PET acquisition. Indeed, inflation can decrease uptake, while increased blood flow can increase

uptake.<sup>32,33</sup> In our study, patients were scanned during shallow breathing and not at full inspiration as required for the diagnosis of lung fibrosis. Yet all patients received a HR-CT scan beforehand, performed according to the guidelines,<sup>34</sup> which is the gold standard imaging technique for the detection of this pathological process. Furthermore, most of the patients were on

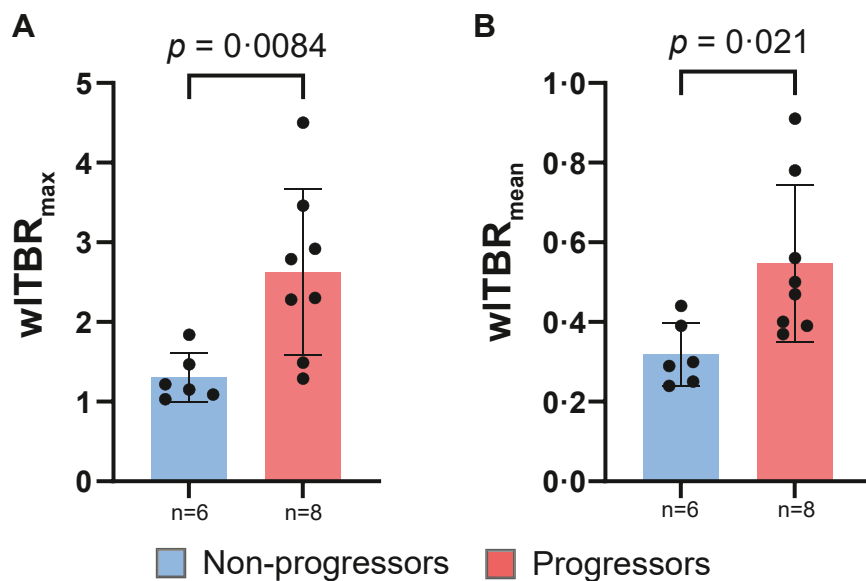


**Fig. 5: Baseline pulmonary FAPI-uptake in relation to non-progressive and progressive IIM-ILD.** Whole-lung maximum (A) and mean (B) target-to-background ratios of patients with IIM-ILD stratified by non-progressive (n = 6) and progressive (n = 8) IIM-ILD within one year. Abbreviations:  $wITBR_{max}$ , whole-lung maximum target-to-background ratio;  $wITBR_{mean}$ , whole-lung mean target-to-background ratio.

ongoing immunosuppressive or antifibrotic therapy, which may have had an effect on FAPI-uptake. We used ILD progression in the previous year as a surrogate to divide patients into progressors or non-progressors, but whether progression in the past predicts further progression in the following year as means of disease activity remains unclear and was not investigated in our study. Finally, the control group of elderly pre-TAVI patients was not matched for age and gender. The rationale of selecting this control group was pragmatic and based on availability of a cohort without lung involvement and images performed at the same PET-unit with the same tracer to ensure consistency and reliability. Alternative controls, such as oncological patients were considered, but ultimately rejected due to the potential presence of pulmonary lesions which would have introduced confounding factors. We carefully excluded controls with morphological CT changes or signs of cardiac decompensation. Despite their older age, which might suggest potential age-related variations in FAPI uptake, it is noteworthy that the control individuals demonstrated FAPI-uptake values comparable to those observed in non-ILD myositis patients. On this basis, we hypothesize that age-related changes or comorbidities in the control group did not significantly influence the direction and magnitude of SUV measurements.

Patients with progressive ILD, which we defined as having an increase in respiratory symptoms, progression in HR-CT, deterioration in PFTs based on current recommendations,<sup>23</sup> and/or escalation of therapy within one year had significantly higher whole-lung FAPI-uptake at baseline. This raises the question as to whether quantification of fibroblast activation by [<sup>68</sup>Ga]<sup>68</sup>Ga-DATA5m.SA.FAPI-PET/CT imaging might improve prediction of the clinical course of individuals with IIM-ILD and thus might be used as a non-invasive imaging technique for risk stratification. These implications in clinical decision-making will have to be confirmed in further prospective studies. Additional studies with longer follow-up periods are required to confirm the prognostic relevance of FAPI for personalised and dynamic disease monitoring in patients with IIM-ILD.

#### Contributors

All authors critically reviewed and approved the final manuscript. KK, TSN and PM had access to the data, verified the underlying study data, controlled the decision to publish and accept full responsibility for the finished work of the study. PM is the guarantor of the study. KK: planning and conception of the study, interpretation of results, data extraction, manuscript draft and preparation, figure development. TSN: planning and conception of the study, FAPI-derived SUV calculation, interpretation of results, manuscript preparation. OCK: planning and conception of the study, FAPI-derived SUV calculation, interpretation of results, manuscript preparation. IG: interpretation of results, manuscript preparation. ES: interpretation of results, manuscript preparation, figure development. DM: interpretation of results, manuscript preparation, figure development. MB: interpretation of results, manuscript preparation, figure development. HPK: interpretation of results, manuscript preparation, figure development. FP:

HR-CT scoring, interpretation of results, manuscript preparation, figure development. HP: HR-CT scoring, interpretation of results, manuscript preparation, figure development. DA: interpretation of results, manuscript preparation, figure development. WL: manuscript preparation, figure development. TTW: manuscript preparation, figure development. SB: interpretation of results, manuscript preparation, figure development. HR: planning and conception of the study, interpretation of results, manuscript preparation, figure development. MH: planning and conception of the study, interpretation of results, manuscript preparation, figure development. PM: planning and conception of the study, interpretation of results, manuscript draft and preparation, figure development.

#### Data sharing statement

All data relevant to the study are included in the article or uploaded as online [Supplementary information](#). A de-identified data set including participants-related data can be provided to researchers upon reasonable request or rather after submission of a project proposal, which can be submitted to the corresponding author.

#### Declaration of interests

KK reports honoraria for lectures and presentations from UCB Pharma, Boehringer Ingelheim, Eli Lilly and AbbVie; support for attending meetings and/or travel: AbbVie, AstraZeneca and Bristol-Myers Squibb. ES reports support for attending meetings and/or travel from Pfizer, Bristol-Myers Squibb, Boehringer-Ingelheim and AstraZeneca. DM reports honoraria from AstraZeneca and travel support from Pfizer. MB received grants from GSK. HP received grants from Siemens, Boehringer-Ingelheim and AstraZeneca; reported honoraria for lectures and presentations from Boehringer-Ingelheim, AstraZeneca and Roche, and participation on a data safety monitoring board/advisory board for Siemens and Boehringer-Ingelheim. DA received grants, speaker fees, or consultancy fees from Abbvie, Gilead, Galapagos, Eli Lilly, Janssen, Merck, Novartis, Pfizer, Sandoz, and Sanofi. HR reports honoraria for lectures and presentations from Gilead, Merck and Pfizer; support for attending meetings and/or travel from Janssen. TSN, OCK, IG, HPK, FP, WL, TTW, SB, MH, and PM declare no competing interests.

#### Acknowledgements

This work was supported by the Austrian Research Fund (FWF) to P.M. 15620-B. We thank all patients who volunteered to take part in the study.

#### Appendix A. Supplementary data

Supplementary data related to this article can be found at <https://doi.org/10.1016/j.jclineim.2024.102598>.

#### References

- Lundberg IE, Fujimoto M, Vencovsky J, et al. Idiopathic inflammatory myopathies. *Nat Rev Dis Primers*. 2021;7(1):86.
- Johnson C, Pinal-Fernandez I, Parikh R, et al. Assessment of mortality in autoimmune myositis with and without associated interstitial lung disease. *Lung*. 2016;194(5):733–737.
- Cavagna L, Trallero-Aragués E, Meloni F, et al. Influence of anti-synthetase antibodies specificities on antisynthetase syndrome clinical spectrum time course. *J Clin Med*. 2019;8(11):2013.
- Hallowell RW, Paik JJ. Myositis-associated interstitial lung disease: a comprehensive approach to diagnosis and management. *Clin Exp Rheumatol*. 2022;40(2):373–383.
- Flaherty KR, Wells AU, Cottin V, et al. Nintedanib in progressive fibrosing interstitial lung diseases. *N Engl J Med*. 2019;381(18):1718–1727.
- Satoh M, Tanaka S, Ceribelli A, Calise SJ, Chan EK. A comprehensive overview on myositis-specific antibodies: New and old biomarkers in idiopathic inflammatory myopathy. *Clin Rev Allergy Immunol*. 2017;52(1):1–19.
- Osawa T, Morimoto K, Sasaki Y, et al. The serum ferritin level is associated with the treatment responsiveness for rapidly progressive interstitial lung disease with amyopathic dermatomyositis, irrespective of the anti-MDA5 antibody level. *Intern Med*. 2018;57(3):387–391.

- 8 Zamora AC, Hoskote SS, Abascal-Bolado B, et al. Clinical features and outcomes of interstitial lung disease in anti-Jo-1 positive anti-synthetase syndrome. *Respir Med.* 2016;118:39–45.
- 9 Mehta P, Aggarwal R, Porter JC, Gunawardena H. Management of interstitial lung disease (ILD) in myositis syndromes: a practical guide for clinicians. *Best Pract Res Clin Rheumatol.* 2022;36(2):101769.
- 10 Davidson S, Coles M, Thomas T, et al. Fibroblasts as immune regulators in infection, inflammation and cancer. *Nat Rev Immunol.* 2021;21(11):704–717.
- 11 King TE Jr, Pardo A, Selman M. Idiopathic pulmonary fibrosis. *Lancet.* 2011;378(9807):1949–1961.
- 12 Martinez FJ, Collard HR, Pardo A, et al. Idiopathic pulmonary fibrosis. *Nat Rev Dis Primers.* 2017;3:17074.
- 13 Lindner T, Loktev A, Giesel F, Kratochwil C, Altmann A, Haberkorn U. Targeting of activated fibroblasts for imaging and therapy. *EJNMMI Radiopharm Chem.* 2019;4(1):16.
- 14 Toms J, Kogler J, Maschauer S, et al. Targeting fibroblast activation protein: radiosynthesis and preclinical evaluation of an (18)F-labeled FAP inhibitor. *J Nucl Med.* 2020;61(12):1806–1813.
- 15 Pang Y, Zhao L, Meng T, et al. PET imaging of fibroblast activation protein in various types of cancer using (68)Ga-FAP-2286: comparison with (18)F-FDG and (68)Ga-FAP1-46 in a single-center, prospective study. *J Nucl Med.* 2023;64(3):386–394.
- 16 Schmidkonz C, Rauber S, Atzinger A, et al. Disentangling inflammatory from fibrotic disease activity by fibroblast activation protein imaging. *Ann Rheum Dis.* 2020;79(11):1485–1491.
- 17 Bergmann C, Distler JHW, Treutlein C, et al. <sup>68</sup>Ga-FAPI-04 PET-CT for molecular assessment of fibroblast activation and risk evaluation in systemic sclerosis-associated interstitial lung disease: a single-centre, pilot study. *Lancet Rheumatol.* 2021;3(3):e185–e194.
- 18 Li J, Wei W, Xu W, Wu W, Liu J, Ye S. [(68)Ga]Ga-FAPI-04 and [(18)F]FDG PET/CT in a patient with MDA5 dermatomyositis. *Eur J Nucl Med Mol Imaging.* 2023;50(12):3790–3791.
- 19 Lundberg IE, Tjärnlund A, Bottai M, et al. 2017 European League against Rheumatism/American College of Rheumatology classification criteria for adult and juvenile idiopathic inflammatory myopathies and their major subgroups. *Ann Rheum Dis.* 2017;76(12):1955–1964.
- 20 Connors GR, Christopher-Stine L, Oddis CV, Danoff SK. Interstitial lung disease associated with the idiopathic inflammatory myopathies: what progress has been made in the past 35 years? *Chest.* 2010;138(6):1464–1474.
- 21 Allenbach Y, Mammen AL, Benveniste O, Stenzel W. 224th ENMC international workshop: clinico-sero-pathological classification of immune-mediated necrotizing myopathies zandvoort, The Netherlands, 14–16 October 2016. *Neuromuscul Disord.* 2018;28(1):87–99.
- 22 Carbone RG, Paredi P, Monselise A, Bottino G, Puppo F. New York Heart Association class associated with imaging is a prognostic mortality risk predictor in interstitial lung diseases. *Eur Rev Med Pharmacol Sci.* 2020;24(17):9012–9021.
- 23 Raghu G, Remy-Jardin M, Richeldi L, et al. Idiopathic pulmonary fibrosis (an update) and progressive pulmonary fibrosis in adults: an official ATS/ERS/JRS/ALAT clinical practice guideline. *Am J Respir Crit Care Med.* 2022;205(9):e18–e47.
- 24 Giesel FL, Kratochwil C, Lindner T, et al. (68)Ga-FAPI PET/CT: biodistribution and preliminary dosimetry estimate of 2 DOTA-containing FAP-targeting agents in patients with various cancers. *J Nucl Med.* 2019;60(3):386–392.
- 25 Moon ES, Elvas F, Vliegen G, et al. Targeting fibroblast activation protein (FAP): next generation PET radiotracers using squaramide coupled bifunctional DOTA and DATA(5m) chelators. *EJNMMI Radiopharm Chem.* 2020;5(1):19.
- 26 Goh NS, Desai SR, Veeraraghavan S, et al. Interstitial lung disease in systemic sclerosis: a simple staging system. *Am J Respir Crit Care Med.* 2008;177(11):1248–1254.
- 27 Hansell DM, Bankier AA, MacMahon H, McCloud TC, Müller NL, Remy J. Fleischner society: glossary of terms for thoracic imaging. *Radiology.* 2008;246(3):697–722.
- 28 Lega JC, Reynaud Q, Belot A, Fabien N, Durieu I, Cottin V. Idiopathic inflammatory myopathies and the lung. *Eur Respir Rev.* 2015;24(136):216–238.
- 29 Yang P, Luo Q, Wang X, et al. Comprehensive analysis of fibroblast activation protein expression in interstitial lung diseases. *Am J Respir Crit Care Med.* 2023;207(2):160–172.
- 30 Rosenkrans ZT, Massey CF, Bernau K, et al. [(68) Ga]Ga-FAPI-46 PET for non-invasive detection of pulmonary fibrosis disease activity. *Eur J Nucl Med Mol Imaging.* 2022;49(11):3705–3716.
- 31 Egger C, Cannet C, Gérard C, et al. Effects of the fibroblast activation protein inhibitor, PT100, in a murine model of pulmonary fibrosis. *Eur J Pharmacol.* 2017;809:64–72.
- 32 Broens B, Zwezerijnen BGJC, van der Laken CJ, Voskuyl AE. Quantification of <sup>68</sup>Ga-FAPI-04 in systemic sclerosis-associated interstitial lung disease. *Lancet Rheumatol.* 2021;3(7):e475.
- 33 Chen DL, Cheriyan J, Chilvers ER, et al. Quantification of lung PET images: challenges and opportunities. *J Nucl Med.* 2017;58(2):201–207.
- 34 Lynch DA, Sverzellati N, Travis WD, et al. Diagnostic criteria for idiopathic pulmonary fibrosis: a fleischner society white paper. *Lancet Respir Med.* 2018;6(2):138–153.